

Published: Physical Chemistry Chemical Physics. 2013, 15: 18671-18677. doi:10.1039/C3CP53282H

CO Oxidation on Stepped-Pt(111) under Electrochemical Conditions: Insights from Theory and Experiment

C. Busó-Rogero, E. Herrero*

*Instituto Universitario de Electroquímica, Universidad de Alicante,
Apdo. 99, E-03080 Alicante, Spain*

J. Bandlow, A. Comas-Vives, and Timo Jacob*

*Institut für Elektrochemie, Universität Ulm,
Albert-Einstein-Allee 47, D-89069 Ulm, Germany*

Abstract

The co-adsorption of CO and OH on two Pt stepped surfaces vicinal to the (111) orientation has been evaluated by means of density functional theory (DFT) calculations. Focusing on Pt(533) and Pt(221), which contain (100) and (111)-steps, respectively, we find that (111)-steps are more reactive towards CO oxidation than surfaces containing (100)-steps. The DFT results are compared with electrochemical experiments on the CO adsorption and oxidation on these vicinal surfaces.

Keywords: CO oxidation, CO/OH Co-adsorption, Pt-stepped surfaces, Density Functional Theory

*corresponding authors: herrero@ua.es, timo.jacob@uni-ulm.de

1. Introduction

Improving the catalytic performance of electrochemical reactions and designing new and more efficient catalysts requires a deep knowledge of how and where the reaction is taking place on a given electrode. To gain such knowledge, the reaction must be studied under very controlled conditions, so that the mechanism and the effects of different environmental parameters can be untangled. Since the most important electrochemical reactions are structure-sensitive, many of these model studies involve the use of single crystal electrodes, allowing for a direct comparison to theoretical studies to unravel the reactivity of different surface sites. This finally helps understanding the catalysts' behavior in practical applications.

Of particular importance are stepped surfaces, as they combine terraces of a given orientation with monoatomic-high steps. The steps are composed of atoms with low coordination, which significantly affects their reactivities. Furthermore, in most cases these sites show almost identical behavior as low-coordinated atoms that are present on nanoparticles used in practical electrodes – for particle sizes beyond the quantum-size region. It has been shown that steps often have an important effect on the reactivity of surfaces. For instance, (111)-steps on vicinal Pt(111) surfaces are able to break the C–C bond in the ethanol oxidation reaction, so that the final product is CO₂ and not acetic acid [1-3]; or that CO formation from formic acid only takes place on (111)-steps [4,5].

Among the most studied reactions in electrochemistry, CO adsorption and oxidation occupies a prominent place. Understanding this reaction is very important for fundamental electrochemistry but also for fuel

cell research, since CO is involved either as a poison or as an intermediate in the anode reactions. In this way, traces of CO are present in hydrogen steams when being obtained by reforming hydrocarbons. Further, CO is an intermediate in the main or side paths in the oxidation mechanism of formic acid, methanol and ethanol [6,7]. Although our knowledge of the CO oxidation mechanism has improved over the last years, there are still many unsolved issues.

The oxidation kinetics of adsorbed CO on Pt single crystal-electrodes has been extensively studied both in the absence [8-18] and in the presence of dissolved CO in acidic solutions [19-22]. These studies have revealed that the CO oxidation on Pt(111) and vicinal electrodes takes place according to the mean field Langmuir–Hinselwood (L–H) mechanism [10,11,14,16], in which adsorbed CO reacts with an adsorbed OH species originating from waters' dissociative adsorption. Since the oxidation process takes place at very localized sites where OH_{ads} and CO_{ads} species can interact, the mean field L–H-type mechanism is fulfilled only if CO diffusion on the surface is fast [23]. *Ab initio* results for the CO electro-oxidation on Pt(111) have also proposed that adsorbed OH oxidizes CO molecules [24-26].

It has also been observed that steps play a critical role in oxidation processes. An extrapolation of the rate constants for the CO_{ads} oxidation obtained with Pt(111) vicinal electrodes to the “ideal” (defect-free) Pt(111) electrode indicates that the oxidation on real Pt electrodes is expected to take place almost exclusively at defect (or low-coordinated) sites [16]. Further, studies in basic solutions indicate that CO mobility under those conditions must be slow. Whereas in acidic media, only one oxidation peak is found in the oxidation voltammogram, two or even three peaks appear in basic solutions [27], depending on the

different type of sites present on the surface. Thus, the peak corresponding to CO oxidation on (111)-steps in alkaline media appears at lower potentials than on (100)-steps or on (111) terraces [28,29]. This clearly indicates that the reactivity of steps is indeed different depending on their symmetry. Here, adsorbed OH should play a very significant role on the overall process, since CO oxidation requires the presence of OH on the surface. Regarding this issue, UHV experiments have shown that the properties and adsorption energies of OH/O depends on the step symmetry [30-33].

In this manuscript, our aim is to study the process of OH and CO adsorption on stepped Pt surfaces vicinal to the (111) orientation by means of density functional theory (DFT) and comparing the energetics to experimental studies on the CO electro-oxidation process on Pt stepped electrodes.

2. Methods: DFT Calculations and Experimental Details

DFT energies for the different Pt surfaces were evaluated using the SeqQuest code [34] with localized basis sets represented by a linear combination of optimized "double- ζ plus polarization" contracted Gaussian functions and norm-conserving pseudopotentials, including nonlinear core corrections. The PBE-GGA functional was employed to approximate exchange and correlation energies. The Pt(111) terrace as well as both step edges were modeled by unsymmetric seven-layer slabs. Integrations in reciprocal space were performed on 10×10 (terraces) and 5×10 (steps) Monkhorst-Pack k -point meshes. As models for stepped Pt(111) we used Pt[4(111) \times (100)] and Pt[4(111) \times (111)] surfaces, thus for both surfaces steps are separated by four-atom wide terraces, corresponding to Pt(533) and Pt(221) vicinal surfaces, respectively. With both surfaces we concentrated on the low-coverage limit by using surface unit cell with two step-edge atoms (two times the unit cells shown in Fig. 1). For the separate adsorption of CO (or OH) placing one adsorbate in the unit cell leads to a coverage of 0.50 SML (SML – step-edge monolayers) or ~ 0.125 ML (per entire unitcell). Consequently, coadsorption of CO+OH resulted in coverages of twice these values. We also investigated higher coverages, which, however, showed strong adsorbate-adsorbate repulsion. Binding energies of CO and OH were referenced to the molecules in gas-phase, where positive values indicate strong binding.

The protocol and reagents for the electrochemical experiments have already been described in Ref. [35]. In summary, single crystal electrodes were flame-annealed, cooled down in a $H_2 + Ar$ atmosphere and protected by a water film [36]. It has been shown that this treatment leads to surfaces with topographies close to the nominal [37].

3. Results and Discussion

3.1. CO adsorption on stepped Pt(111) surfaces.

The presence of steps on the (111) terrace modifies the surface stability and its properties, such as the work function

or the potential of zero charge, which was found to be directly proportional to the step density [38-40]. This linear relationship normally breaks up for surfaces with narrow terraces [40], where the perturbation generated by the presence of steps extends over the whole terrace, and step-step interactions may appear. Thus, the behavior of these surfaces no longer can be considered as the sum of step and terrace contributions. Therefore, we always have to compare with the behavior of the perfect (111) surfaces without steps. Therefore, CO adsorption was studied on planar Pt(111) and both types of stepped surfaces, *i.e.* (100) and (111)-steps. Table 1 shows the calculated CO adsorption energies on the different sites of the (111) terrace. Four different adsorption geometries have been considered: atop, bridge, fcc, and hcp sites. We find very similar adsorption energies at all four sites. Indeed, CO adsorption on Pt surfaces is indeed a non-trivial system to be calculated with DFT in general as the approach usually tends to overestimate the 3-fold hollow sites over atop sites, which in low temperature experiments were found to be preferred. As our aim is to investigate the co-adsorption of CO and OH, here we point the reader to the extensive discussions about the so-called "CO/Pt(111) puzzle" [41-53].

Our results indicate that at low coverages the CO adsorption on the terrace has no preferential adsorption site (due to similar binding energies), which is comparable to the findings already reported in literature [41-53]. However, the exact geometry of the adsorption certainly depends on various additional factors, such as coverage and lateral interactions between adsorbed CO molecules.

In electrochemical environments, CO forms different structures on the Pt(111) electrodes [54], which usually combines CO at various surface sites (*e.g.* atop, bridge, multi-bonded positions, and even combinations of these [54]), providing a clear indication that the adsorption energies are indeed very similar at the different surface sites. In order to cover the effects induced by the electrode potential on the systems, different groups performed DFT studies on the CO adsorption on Pt(111) under the influence of a constant electric field [55-57], concluding that the preferred CO adsorption position changes from atop to fcc under decreasing external electric field [55,56].

For stepped surfaces, various possible adsorption sites above and below the step-edge have been considered (see Fig. 1): atop sites (T1 to T4 sites), two different bridge geometries, corresponding to the situations in which the two atoms are in the same atomic row (A sites) or in different ones (B sites), and the fcc and hcp geometries (F and H sites, respectively). Additionally, other adsorption geometries have been studied when the adsorbates are located on sites defined by the atoms on the step edge and the first row of atoms of the Pt(111) terrace underneath. For the (100)-step, we additionally evaluated StBr, StCe and H-1 sites, depending on the adsorbate position, namely on a bridge position, on the center of the (100) step-edge or on an hcp site, respectively. For the (111)-steps the corresponding F-1 site was evaluated, which corresponds to the fcc site formed

between one atom of the step-edge and two Pt atoms of the Pt(111) terrace underneath.

All binding energies are summarized in Table 2 and Table 3. Missing values indicate unstable surface sites, since the adsorbed species relaxed during the optimization to other positions. The obtained adsorption energies clearly show that binding of CO on the step edge is favored with respect to the terrace sites by roughly 0.3–0.4 eV. Although the qualitative picture for the two stepped surfaces is similar, quantitative differences are observed. Thus, for the (100)-step, the most favorable adsorption site on the step corresponds to a bridge position between two Pt atoms on the step-edge (Fig. 2B) although the atop T1 site is similar in energy in agreement with previous DFT results [41,58]. On the (111)-step CO binds to only one Pt atom (Fig. 2A) as already reported by previous *ab initio* calculations [41,58,59,60]. This latter site correspond to a geometry in which the C–O bond is normal not to the (111)- but the (221)-plane.

The results presented here are in good agreement with experimental findings obtained for the Pt electrodes vicinal to the (111) plane. In acid media, it has been proposed that the CO mobility is very high [10]. Thus, CO should always occupy the energetically most favorable sites. For stepped electrodes vicinal to the (111) plane, it is possible to identify the adsorption site of a species using voltammetry. Hydrogen adsorption–desorption processes on step sites give a characteristic peak at 0.27 and 0.13 V for the (100)- and (111)-steps, respectively. For partial CO coverages, even at very low values, the characteristic peak corresponding to the step sites disappears, indicating that CO preferentially occupies step sites. This effect can be observed in Fig. 3, where a partial CO stripping experiment has been carried out. By choosing the appropriate upper potential limit, CO is stripped slowly from the surface. As can be seen, the peak corresponding to the adsorption of hydrogen on the step sites is only recovered in the final stages of the oxidation, that is, when the CO coverage is very low. Additionally, it can be observed that the hydrogen adsorption peak on the (100)- and (111)-steps shifts towards positive potentials in the latter stages of the stripping process. This shift is very similar to that observed for other species adsorbed in the upper part of the step, such as selenium [61]. The change in the peak potential clearly indicates a change in adsorption energy due to either a modification in the energetics of the step or lateral interactions.

The adsorption geometries have also been determined using Fourier-Transformed Infrared-Spectroscopy (FTIR), both in acid and alkaline media [62,63], which indicates that this adsorption geometry is not strongly affected by the electrode potential. The adsorption geometry on the step has been obtained by comparing the FTIR spectra of CO on the stepped surface before and after blocking the step site with Bi. From the difference spectra, it was found that on the (100)-step CO preferentially occupies bridge sites, whereas on the (111)-step site, adsorption at top sites was found.

3.2. OH adsorption on stepped Pt(111) surfaces.

Adsorbed OH is very important for CO oxidation, since the oxidation mechanism takes place according to a Langmuir–Hinshelwood mechanism. For that reason, OH adsorption was also studied on the (111) plane and on stepped surfaces (Table 1–Table 3). On the (111) terraces, adsorption of OH at top and fcc sites has similar energies, whereas it was not possible to obtain a stable configuration for the other two types of surface sites (*i.e.* hcp-hollow and bridge).

In both cases OH adsorbs on a bridge-position (see Fig. 4) between two Pt atoms of the step-edge (A1 site), the nature of the step causing the adsorption energies being roughly 0.3–0.4 eV higher for the (100)-step compared to the (111)-step. Also, there is a large increase in the adsorption energies of ~0.5eV for the (111)-step and ~0.8 eV for the (100)-step compared to the planar Pt(111) surface.

These results have to be compared to the CV measurements obtained for the stepped surfaces (see Fig. 3). For Pt(111) electrodes, the onset for OH adsorption is 0.6 V in perchloric acid solutions. For the stepped surfaces with (111)-steps, there is not a clear indication where the adsorption of OH on the step takes place, since it probably occurs in the region where H adsorption on the terrace takes place. This latter signal is large and for that reason, masks the small contribution from OH adsorption on the step. However, on the Pt(110) surface, which can be also considered as the stepped surface Pt[2(111)×(111)], OH adsorption takes place at ca. 0.2 V, as indicated by the CO displacement technique [40], in good agreement with the difference in adsorption energy found here. For the adsorption on the (100)-step, the major problem is that the step adsorption is a competitive process, in which the H adsorption process is coupled with the OH desorption and vice versa. For that reason, the onset potential depends on the energy of adsorption on the step of both hydrogen and OH, not allowing for a direct comparison to the present calculations.

3.3. CO and OH co-adsorption on the stepped Pt(111) surfaces

Afterwards investigating the independent adsorption of CO and OH, we finally studied the co-adsorption of both species on both types of steps. The results are summarized in Table 4–Table 5. The most stable configurations are shown in Fig. 5. As can be seen, significant differences are observed between both step-edges and with the previous results obtained for each species adsorbing separately. First of all, on both steps the calculated energy for the most stable configurations is 0.1 eV [for (111)-steps] and 0.4 eV [for (100)-steps] lower than the sum of the energies of the most stable configurations for CO and OH separately, indicating certain repulsion between the co-adsorbates. Secondly, the most stable configuration (*i.e.* the preferred binding sites) for the co-adsorbed CO+OH system changes as well. These differences are a consequence of the modification of the local

electronic structure of the neighboring atoms when CO or OH are co-adsorbed. Thus, for the surfaces with (100)-steps CO prefers the F2 site (fcc adsorption site on the Pt(111) terrace), while OH adsorbs on the A1 site (bridge site along the step-edge).

On the other hand, the most stable combination for surfaces with (111)-steps has both CO and OH co-adsorbed at F-1 positions, with an overall binding energy of 4.77 eV. In this configuration both CO and OH are bonded to one Pt atom (Fig. 5) along the step-edge, As has been shown experimentally in Fig. 3, the potential for hydrogen adsorption/desorption on the step changes when CO is additionally present on the step, reflecting alterations in the adsorption sites on the step neighboring the adsorbed CO. Thus, the presence of adsorbed CO (or OH) modifies the adsorption energy of the adjacent surface sites.

From the results presented here, none of the adsorption processes clearly predominates. For the stepped surfaces with (100)-steps, OH remains on the same adsorption site (A1) but CO can be adsorbed at different positions (*e.g.* A1, A3, H2 and T2) without changing the overall binding energy of the CO/OH system: 4.9–5.0 eV.

Concerning the surfaces with (111)-steps, the opposite situation is found, since the most stable adsorption site for a single CO is kept (F-1), while OH can be adsorbed either on the A1 or F-1 position with again similar binding energies for the CO+OH systems: 4.77 and 4.74 eV, respectively

The different behavior of the two stepped surfaces for the co-adsorption of CO+OH necessarily implies a different reactivity. For the reaction between OH and CO, significant differences have been found experimentally, both in acid and alkaline media. In acid media, where it has been proposed that the mobility of CO is very high, the rate constant for CO oxidation in the presence of (111)-steps is always higher than in the presence of (100)-steps [64]. This implies that the presence of the (111)-steps is more effective in the electrocatalytic CO oxidation process. These results are in agreement with the studies presented here. First of all, the adsorption of OH on the steps is always energetically more favorable than the adsorption on the terrace, and for that reason, the CO oxidation process is catalyzed by the presence of steps. Regarding the differences between the reactivity of the two steps, CO and OH are on neighboring sites in the most stable configuration for the surfaces having (111)-steps, so that the reaction between the two species is facilitated. Also, the next stable combination involves the CO on the F-1 position, while OH is adsorbed on the A1 position. As already mentioned, this combination has a binding energy of 4.74 eV. Note that this was expected to be the most stable combination according to the reported single adsorption energies of the CO and OH species (see Tab. 3).

On the other hand, in the most stable configuration CO and OH are at distant positions when (100)-steps are present on the surface, so that a direct reaction is not feasible. For the reaction to take place on the surface with (100)-steps, either CO or OH should diffuse over the surface to neighboring sites, which implies reaching a less stable

configuration. In fact, the following most stable combinations are also involving the OH species adsorbed on the A1 position, while CO is adsorbed on the A3 (bridge-site on the terrace), H2 (hcp site on the terrace) and T2 (atop site on the Pt(111) terrace) positions with binding energies of 4.99, 4.95 and 4.94 eV, respectively. From all these combinations the one in which CO and OH are closest each other corresponds to the one where the CO is adsorbed on the T2 position. The binding energy of this structure is 4.94 eV. Thus, from all the other possible combinations with energies close to the most stable configuration, in only one of them CO and OH are close to react. Further, diffusion of CO is always energetically more favorable than the diffusion of OH, since in all the very stable configurations, OH is adsorbed atop of the step-edge. Also, when CO is diffusing over the surface, the energetically most favorable configurations always implies a CO close to the adsorbed OH for surface with (111)-steps, whereas with (100)-steps three out of four configurations imply a CO molecule far from the OH species. Hence, both our reported theoretical and experimental data suggests that surfaces containing (111)-steps are expected to be more reactive towards CO oxidation than surfaces containing (100)-steps.

4. Summary and Outlook

The adsorption energies of CO, OH, and CO+OH on planar Pt(111) and vicinal surfaces containing (111)- or (100)-steps have been evaluated by means of DFT. Our results show that the binding for the co-adsorption of CO and OH on the (100)-steps is stronger than in the presence of (111)-steps. For OH adsorption, the difference in adsorption energy between (111) terrace sites and steps are in agreement with that found in electrochemical environments with voltammetry. In the case of CO, the experimental assignment of the adsorption geometry for CO adsorbed on the step site is corroborated by the DFT calculations. The highest adsorption energy for the co-adsorbance of CO and OH on the (100)-step is 5.02 eV, while the most likely reactive configuration has a slightly lower binding energy of 4.94 eV. In the latter structure the OH is on the bridge site of the step-edge, while CO occupies the T2-site, which corresponds to an atop position close to the step-edge (where OH is adsorbed). For the case of (111)-steps binding energies are lower. Here, the most stable configuration is where both reactants are located at fcc sites (F-1) in front of (but underneath) the step-edge, having an overall binding energy of 4.77 eV. These results are in agreement with the experimental data, in which a different behavior of the (111) and (100)-steps for CO adsorption and oxidation has been found. Also, the adsorption geometries of CO on the step sites,

5. Acknowledgements

This work has been supported by the European Union through the Marie-Curie-ITN ELCAT. J.B., A.C.-V. and T.J. gratefully acknowledge support from the "Deutsche

Published: Physical Chemistry Chemical Physics. 2013, 15: 18671-18677. doi:10.1039/C3CP53282H

Forschungsgemeinschaft (DFG) as well as by the bwGRiD for computing resources. Further, support from the European Research Council through the ERC-StG THEOFUN is gratefully acknowledged. E.H and C. B.-R. also

acknowledge the support from MICIN (project No. CTQ2010-16271)

6. Figures

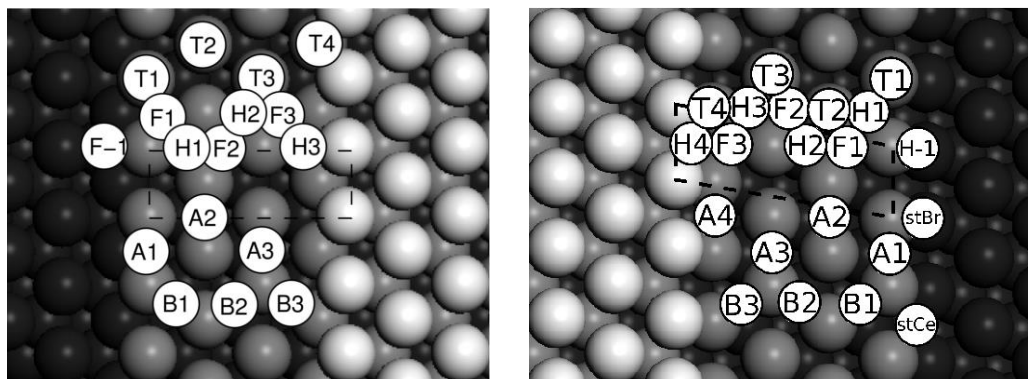


Figure 1: Hard-sphere models of the Pt(221) (left) and Pt(533) (right) surface, which served as model systems to investigate adsorption on (111)- and (100)-steps, respectively. The (1×1) surface unit cells are indicated by a dashed box, while all sites at which adsorption has been studied are labeled.

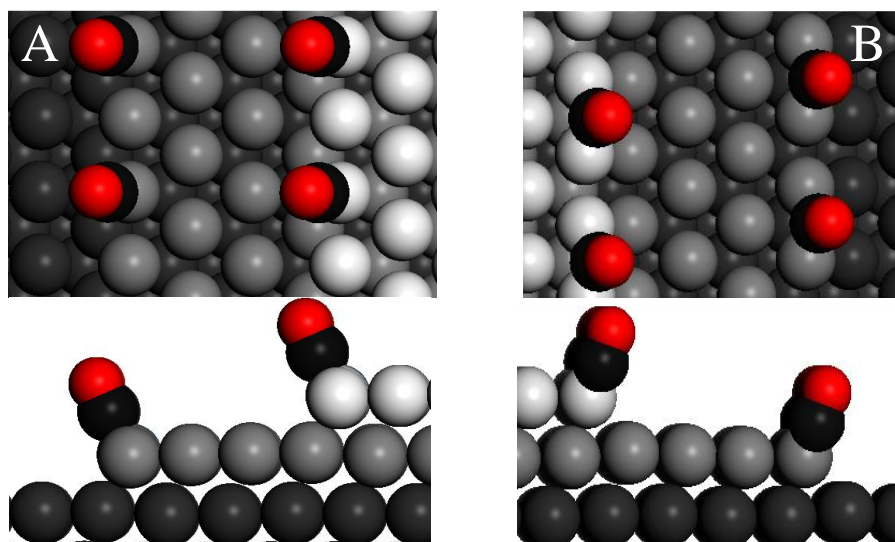


Figure 2: Optimized structure for CO adsorbed on the most stable adsorption site of Pt(221) (A) and Pt(533) (B). Top panels show the top view, while bottom panels are the corresponding side views..

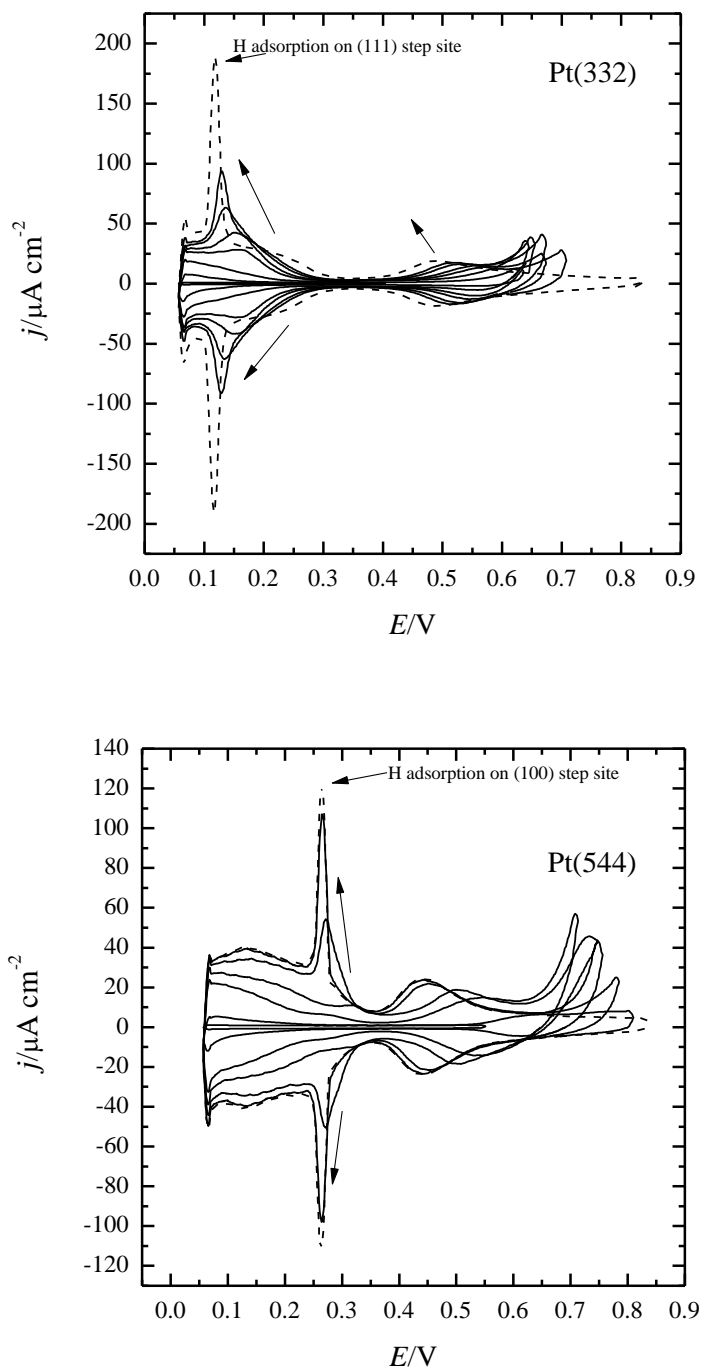


Figure 3. Partial CO stripping on the Pt(332) and Pt(544) electrodes in 0.5 M H₂SO₄. Potential values are with respect to the reversible hydrogen electrode (RHE). Arrows indicate the evolution of the voltammetric profile upon diminution of the CO coverage. The final voltammograms after complete removal of CO is shown in dashed lines. Only selected scans have been shown to improve clarity of the figure.

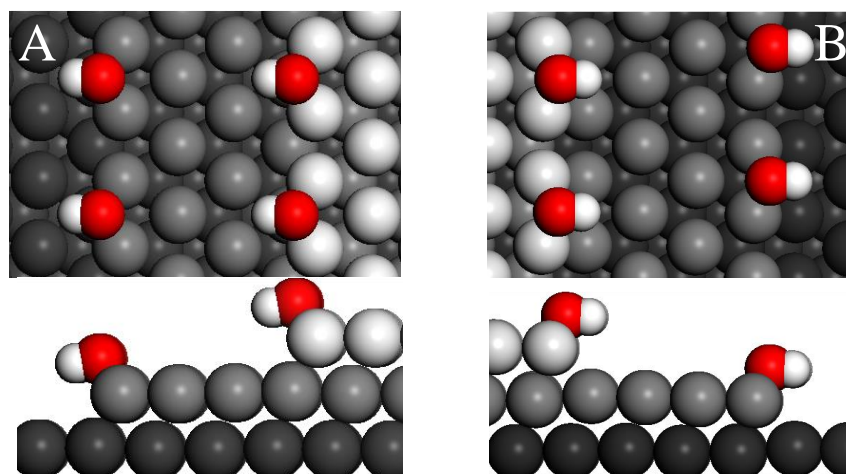


Figure 4: Optimized structure for OH adsorbed on the most stable adsorption site of Pt(221) (A) and Pt(533) (B). Top panels show the top view, while bottom panels are the corresponding side views.

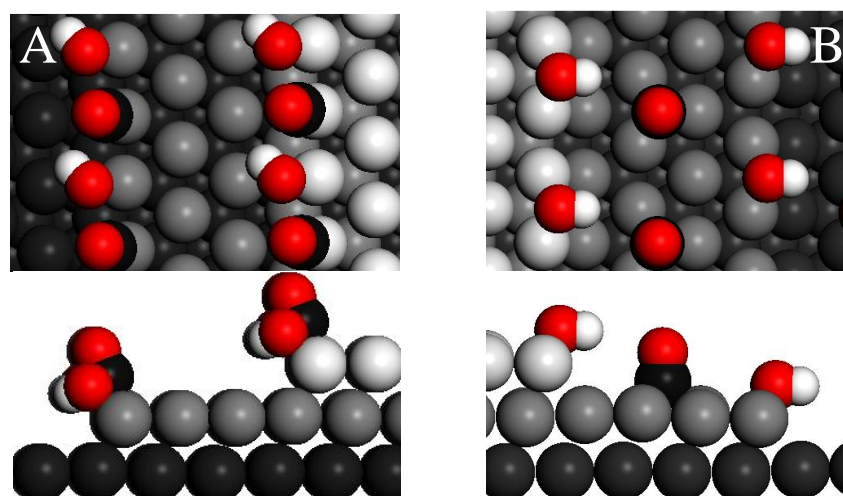


Figure 5: Optimized structure for co-adsorption of CO and OH in the most stable configurations on Pt(221) (A) and Pt(533) (B). Top panels show the top view, while bottom panels are the corresponding side views.

7. Tables

Table 1: Adsorption energies (in eV) of CO and OH single adsorption on the (111) terrace.

Adsorption site	$E_{\text{bind}}^{\text{OH}}$ [eV]	$E_{\text{bind}}^{\text{CO}}$ [eV]
2×2 top	2.44	1.64
2×2 bridge	–	1.68
2×2 fcc	2.46	1.67
2×2 hcp	–	1.66

Table 2: Adsorption energies (in eV) of CO and OH single adsorption on the (100)-step, *i.e.* Pt(533) vicinal surface.

Adsorption site	$E_{\text{bind}}^{\text{OH}}$ [eV]	$E_{\text{bind}}^{\text{CO}}$ [eV]
A1	3.29	2.11
A2	2.45	1.62
A3	2.46	1.68
A4	–	–1.79
B1	–	1.58
B2	–	1.67
B3	–	1.52
F1	–	1.59
F2	–	1.69
F3	–	1.46
H1	–	–
H-1	2.74	1.97
H2	–	1.63
H3	1.44	1.58
H4	–	–1.79
T1	2.75	2.00
T2	2.37	1.61
T3	2.40	1.62
T4	2.30	1.79

Table 3: Adsorption energies (in eV) of CO and OH single adsorption on different positions on the (111)-step, *i.e.* Pt(221) vicinal surface.

Adsorption site	$E_{\text{bind}}^{\text{OH}}$ [eV]	$E_{\text{bind}}^{\text{CO}}$ [eV]
A1	2.92	1.94
A2	1.15	1.63
A3	2.35	1.62
A4	–	–
B1	–	–
B2	2.30	1.66
B3	–	–
F1	–	–
F-1	2.74	2.02
F2	–	–
F3	–	1.93
H1	–	–
H2	–	1.61
H3	–	–
T1	2.79	–
T2	2.35	1.57
T3	2.39	1.53
T4	–	–

Table 4: Adsorption energies (in eV) of CO + OH co-adsorbed on different positions on the (100)-step, *i.e.* Pt(533) vicinal surface.

CO site	OH site	$E_{\text{bind}}^{\text{CO+OH}}$ [eV]
A1	A1	4.9
A1	A2	4.62
A1	A3	4.6
A1	T2	4.55
A1	T3	4.54
A1	T4	4.66
A3	A1	4.99
F2	A1	5.02
H2	A1	4.95
T1	A1	4.61
T2	A1	4.94
T3	A1	4.88
T4	A1	4.79

Table 5: Adsorption energies (in eV) of CO + OH co-adsorbed on different positions on the (111)-step, *i.e.* Pt(221) vicinal surface.

CO site	OH site	$E_{\text{bind}}^{\text{CO+OH}}$ [eV]
F-1	F-1	4.77
F-1	A2a	–
F-1	A2b	4.30
F-1	A3	4.37
F-1	T2	4.46
F-1	T3	4.42
F-1	T4	4.40
A3	A1	4.62
F2	A1	–
H2	A1	–
F-1	A1	4.74
T2	A1	4.51
T3	A1	4.41

8. References

- ¹ D. J. Tarnowski, C. Korzeniewski, *J. Phys. Chem. B*, 101 (1997) 253.
- ² F. Colmati, G. Tremiliosi, E. R. Gonzalez, A. Berna, E. Herrero, J. M. Feliu, *Phys. Chem. Chem. Phys.*, 11 (2009) 9114.
- ³ J. Souza-Garcia, E. Herrero, J. M. Feliu, *Chem. Phys. Chem.*, 11 (2010) 1391.
- ⁴ M. D. Maciá, E. Herrero, J. M. Feliu, *Electrochim. Acta*, 47 (2002) 3653.
- ⁵ V. Grozovski, V. Climent, E. Herrero, J. M. Feliu, *Phys. Chem. Chem. Phys.*, 12 (2010) 8822.
- ⁶ R. Parsons, T. Vandernoot, *J. Electroanal. Chem.*, 257 (1988) 9.
- ⁷ W. Gao, J. E. Mueller, Q. Jiang, T. Jacob, *Angew. Chem. Int. Ed.*, 51 (2012) 9448.
- ⁸ B. Love, J. Lipkowski, *ACS Symp. Ser.*, 378 (1988) 484.
- ⁹ L. Palaikis, D. Zurawski, M. Hourani, A. Wieckowski, *Surf. Sci.*, 199 (1988) 183.
- ¹⁰ M. Bergelin, E. Herrero, J. M. Feliu, M. Wasberg, *J. Electroanal. Chem.*, 467 (1999) 74.
- ¹¹ N. P. Lebedeva, M. T. M. Koper, J. M. Feliu, R. A. van Santen, *J. Electroanal. Chem.*, 524 (2002) 242.
- ¹² E. Santos, E. P. M. Leiva, W. Vielstich, *Electrochim. Acta*, 36 (1991) 555.
- ¹³ N. M. Marković, T. J. Schmidt, B. N. Grgur, H. A. Gasteiger, R. J. Behm, P. N. Ross, *J. Phys. Chem. B*, 103 (1999) 8568.
- ¹⁴ E. Herrero, J. M. Feliu, S. Blais, Z. Radović-Hrapović, G. Jerkiewicz, *Langmuir*, 16 (2000) 4779.
- ¹⁵ E. Herrero, B. Alvarez, J. M. Feliu, S. Blais, Z. Radović-Hrapović, G. Jerkiewicz, *J. Electroanal. Chem.*, 567 (2004) 139.
- ¹⁶ N. P. Lebedeva, M. T. M. Koper, J. M. Feliu, R. A. van Santen, *J. Phys. Chem. B*, 106 (2002) 12938.
- ¹⁷ B. Pozniak, Y. Mo, D. A. Scherson, *Faraday Discuss.*, 121 (2002) 313.
- ¹⁸ N. P. Lebedeva, M. T. M. Koper, E. Herrero, J. M. Feliu, R. A. van Santen, *J. Electroanal. Chem.*, 487 (2000) 37.
- ¹⁹ M. T. M. Koper, T. J. Schmidt, N. M. Marković, P. N. Ross, *J. Phys. Chem. B*, 105 (2001) 8381.
- ²⁰ C. A. Angelucci, F. C. Nart, E. Herrero, J. M. Feliu, *Electrochem. Commun.*, 9 (2007) 1113.
- ²¹ C. A. Angelucci, E. Herrero, J. M. Feliu, *J. Solid State Electrochem.*, 11 (2007) 1531.
- ²² P. Strasser, M. Eiswirth, G. Ertl, *J. Chem. Phys.*, 107 (1997) 991.
- ²³ A. V. Petukhov, W. Akemann, K. A. Friedrich, U. Stimming, *Surf. Sci.*, 402 (1998) 182.
- ²⁴ S. Desai, M. Neurock, *Electrochim. Acta*, 48 (2003) 3759.
- ²⁵ M. J. Janik, M. Neurock, *Electrochim. Acta*, 52 (2007) 5517.
- ²⁶ M. J. Janik, C. Taylor, M. Neurock, *Top. Catal.*, 46 (2007) 306.
- ²⁷ G. Garcia, M. T. M. Koper, *Phys. Chem. Chem. Phys.*, 10 (2008) 3802.
- ²⁸ G. Garcia, M. T. M. Koper, *Phys. Chem. Chem. Phys.*, 11 (2009) 11437.
- ²⁹ G. Garcia, M. T. M. Koper, *J. Am. Chem. Soc.*, 131 (2009) 5384.
- ³⁰ M. van der Niet, O. T. Berg, L. B. F. Juurlink, M. T. M. Koper, *J. Phys. Chem. C*, 114 (2010) 18953.
- ³¹ M. van der Niet, A. den Dunnen, L. B. F. Juurlink, M. T. M. Koper, *J. Chem. Phys.*, 132 (2010).
- ³² M. van der Niet, A. den Dunnen, L. B. F. Juurlink, M. T. M. Koper, *Phys. Chem. Chem. Phys.*, 13 (2011) 1629.
- ³³ M. van der Niet, A. den Dunnen, M. T. M. Koper, L. B. F. Juurlink, *Phys. Rev. Lett.*, 107 (2011).
- ³⁴ C. Verdozzi, P. A. Schultz, R. Q. Wu, A. H. Edwards, N. Kioussis, *Phys. Rev. B*, 66 (2002) 125408.
- ³⁵ V. Grozovski, V. Climent, E. Herrero, J. M. Feliu, *Phys. Chem. Chem. Phys.*, 12 (2010) 8822.
- ³⁶ J. Clavilier, D. Armand, S. G. Sun, M. Petit, *J. Electroanal. Chem.*, 205 (1986) 267.
- ³⁷ E. Herrero, J. M. Orts, A. Aldaz, J. M. Feliu, *Surf. Sci.*, 440 (1999) 259.
- ³⁸ K. B. Besocke, B. Krahl-Urban, H. Wagner, *Surf. Sci.*, 68 (1977) 39.
- ³⁹ S. Trasatti, *Electrochim. Acta*, 36 (1991) 1659.
- ⁴⁰ R. Gómez, V. Climent, J. M. Feliu, M. J. Weaver, *J. Phys. Chem. B*, 104 (2000) 597.
- ⁴¹ P. J. Feibelman, B. Hammer, J. K. Nørskov, F. Wagner, M. Scheffler, R. Stumpf, R. Watwe, J. Dumesic, *J. Phys. Chem. B*, 105 (2001) 4018.
- ⁴² D. Geschke, T. Baştuğ, T. Jacob, S. Fritzsche, W.-D. Sepp, B. Fricke, S. Varga, J. Anton, *Phys. Rev. B*, 64 (2001) 235411.
- ⁴³ P. H. T. Philipsen, E. van Lenthe, J. G. Snijders, E. J. Baerends, *Phys. Rev. B*, 56 (1997), 13556.
- ⁴⁴ Q. M. Hu, K. Reuter, M. Scheffler, *Phys. Rev. Lett.*, 98 (2007), 4.
- ⁴⁵ F. Abild-Pedersen, M. P. Andersson, *Surf. Sci.*, 601 (2007) 1747.
- ⁴⁶ P. Lazić, M. Alaei, N. Atodiresei, V. Caciuc, R. Brako, S. Blugel, *Physical Review B*, 81 (2010) 6.
- ⁴⁷ K. Doll, *Surf. Sci.*, 573 (2004) 464.
- ⁴⁸ I. Grinberg, Y. Yourdshahyan, A.M. Rappé, *J. Chem. Phys.*, 117 (2002) 2264.

- ⁴⁹ S. E. Mason, I. Grinberg, A. M. Rappé, *Physical Review B*. 69 (2004) 161401.
- ⁵⁰ E. D. German, M. Sheintuch, *J. Phys. Chem. C*. 112 (2008) 14377.
- ⁵¹ A. Stroppa, G. Kresse, *New J. Phys.* 10 (2008) 17
- ⁵² W. Liu, Y. F. Zhu, J. S. Lian, Q. Jiang, *J. Phys. Chem. C*. 111 (2007) 1005.
- ⁵³ I. Dabo, A. Wieckowski, N. Marzari, *Journal of the American Chemical Society*. 129 (2007) 11045.
- ⁵⁴ M. W. Severson, C. Stuhlmann, I. Villegas, M. J. Weaver, *J. Chem. Phys.*, 103 (1995) 9832.
- ⁵⁵ M. Mamatkulov, J. S. Filhol, *Phys. Chem. Chem. Phys.* 13 (2011) 7675.
- ⁵⁶ P. Deslahra, E. E. Wolf, W. F. Schneider, *J. Phys. Chem. A*. 113 (2009) 4125.
- ⁵⁷ A.Y. Lozovoi, A. Alavi, *J. Electroanal. Chem.* 607 (2007) 140.
- ⁵⁸ B. Hammer, O. H. Nielsen, J. K. Nørskov, *Catalysis Letters*. 46 (1997) 31.
- ⁵⁹ H. Orita, N. Itoh, Y. Inada, *Surf. Sci.* 571 (2004) 161.
- ⁶⁰ H. Orita, Y. Inada, *The Journal of Physical Chemistry B*. 109 (2005) 22469.
- ⁶¹ E. Herrero, V. Climent, J. M. Feliu, *Electrochem. Commun.*, 2 (2000) 636.
- ⁶² Q. S. Chen, A. Berna, V. Climent, S. G. Sun, J. M. Feliu, *Phys. Chem. Chem. Phys.*, 12 (2010) 11407.
- ⁶³ M.J.S. Farias, E. Herrero, J.M. Feliu, *J. Phys. Chem. C*, 117 (2013) 2903.
- ⁶⁴ Q. S. Chen, J. M. Feliu, A. Berna, V. Climent, S. G. Sun, *Electrochim. Acta*, 56 (2011) 5993.